
DynFrame: Adaptive Reasoning-Driven Multimodal Framework with Dynamic Frame Augmentation for Complex Video Understanding

Peng Zhang^{1,2,*} Guanghao Zhang^{2,*§} Wangui He² Longxiang Zhang² Mushui Liu^{1,2} Yan Xia²
Zhenhao Peng² Weilong Dai² Jinlong Liu² Haobing Tang² Le Zhang² Hao Jiang^{2,†} Pipei Huang²

¹Zhejiang University ²Alibaba Group

Abstract

Recent video multimodal large language models (MLLMs) increasingly couple step-by-step reasoning with on-demand visual evidence retrieval, allowing models to revisit relevant video segments during inference. However, two structural gaps remain in existing thinking-with-video systems. **(i)** Sampling density is not a learnable decision: existing methods may let the model decide *where* to look, but the per-window frame rate is largely fixed. As a result, fine-grained evidence is often recovered through repeated retrieval calls which increases inference context length and training difficulty. **(ii)** Retrieval and answer generation are usually optimized with a single trajectory-level advantage, so the “where to look” tokens and the “how to answer” tokens receive the same credit even when one is correct and the other is not. To address these gaps, we present **DynFrame**, a framework that emits the temporal window and the sampling density as native tokens within a single autoregressive pass, such learnable span–density retrieval enables acquiring multi-granularity evidence with a single retrieval step. Based on the above tokenized retrieval interface, we further introduce **Segment-Decoupled GRPO (SD-GRPO)**, which splits each rollout at the retrieval boundary and assigns role-specific token-level advantages, separately crediting the sampling decision and the answer. Trained on the curated **DM-CoT-74k** and **DM-RL-45k**, DynFrame-4B is competitive with strong 7B–8B baselines across six benchmarks (NEXT-GQA, Charades-STA, ActivityNet-MR, Video-MME, MLVU, LVBench), and DynFrame-8B sets new state-of-the-art on most metrics. Code is available at <https://github.com/zhangguanghao523/DynFrame>.

1 Introduction

Multimodal large language models (MLLMs) [2, 46, 18, 14, 4, 16, 1] have substantially advanced video question answering, temporal grounding, and long-form video understanding [34, 9, 27, 17, 7, 45, 31]. Building on chain-of-thought (CoT) reasoning [33, 25, 32], recent supervised and reinforcement-learning post-training methods further improve multi-step video inference [6, 20, 30]. However, most video reasoners still operate after a fixed visual pass: a sparse set of frames is selected before generation, and all subsequent intermediate steps are purely textual [23, 40, 15, 43, 1]. This design is fragile for long videos, where the answer may hinge on a short action, a brief object state change, or multiple clues scattered across a redundant temporal context. As reasoning chains grow, the model can drift away from the actual visual evidence and hallucinate missing fine-grained events.

*Equal contribution. §Project lead. †Corresponding author.

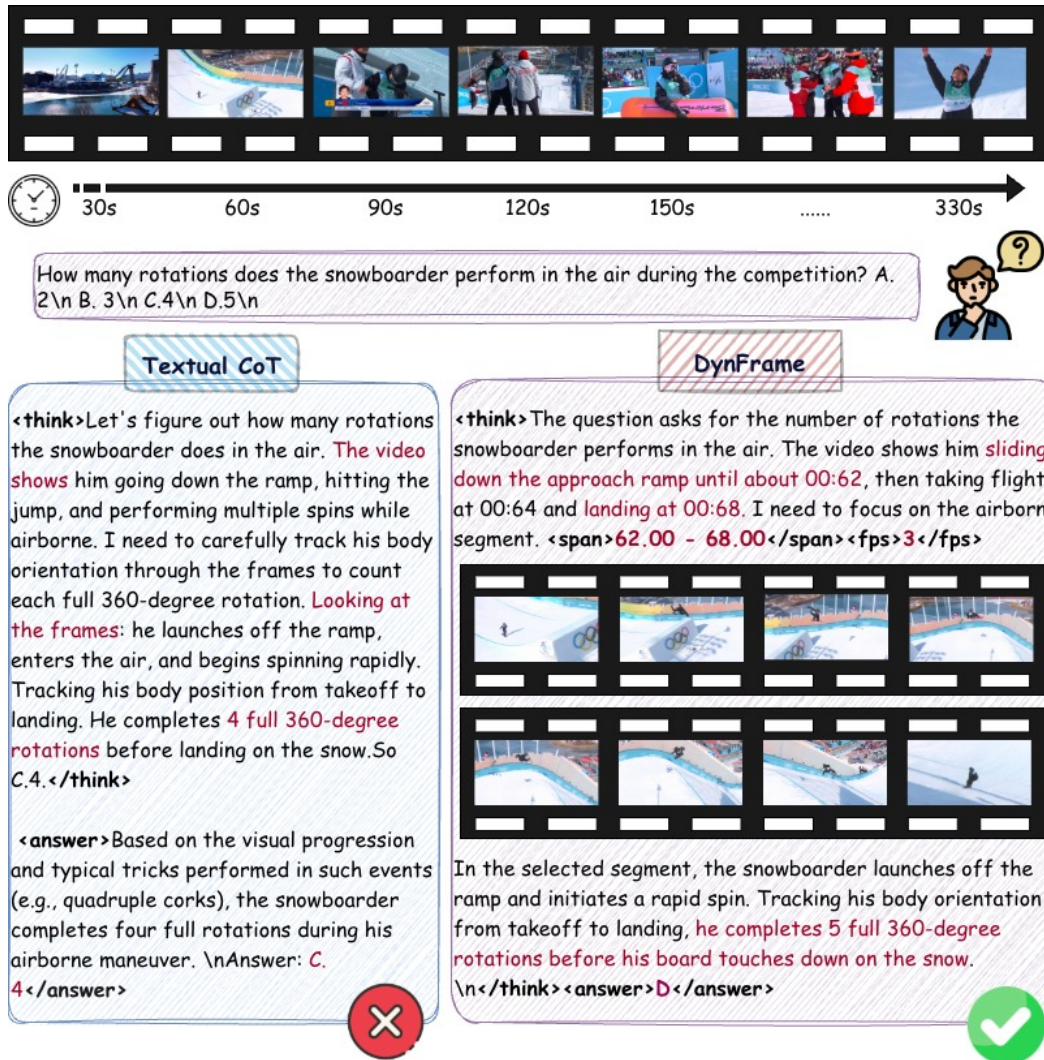


Figure 1: **Textual CoT vs. DynFrame.** Textual CoT (left) reasons over a fixed sparse frame set and misses the airborne segment, yielding a wrong rotation count. DynFrame (right) emits `` and `<fps>` tokens *within* its reasoning to retrieve a denser, temporally focused frame set, and then continues reasoning over the augmented visual context to reach the correct answer.

A growing *thinking-with-video* line of work addresses this limitation by allowing models to actively revisit video evidence during inference. Existing systems instantiate visual revisiting through several retrieval interfaces: tool-based clip retrieval that calls an external module to crop or resample candidate video segments [41, 36], zoom-in or temporal-focusing mechanisms that inspect local regions at higher resolution [8, 5], multi-turn frame spotlighting or iterative perception that progressively refines clue-focused temporal regions [12, 35], and native interleaved tool invocation that couples evidence seeking with reasoning in a shared context [39, 24, 21]. These systems demonstrate the importance of revisiting visual evidence, but fine-grained evidence acquisition is often achieved by issuing repeated retrieval calls, refining temporal clues across turns, or appending additional high-resolution clips into an expanding context. Such multi-turn retrieval increases inference context length and also complicates training. This motivates a complementary question: *can a video MLLM make each retrieval action more expressive, so that task-adaptive, multi-granularity evidence can be acquired with fewer retrieval steps?*

To address these challenges, we introduce **DynFrame**, a novel framework that emits the temporal window and the sampling density as native tokens within a single autoregressive pass, turning frame-rate adaptation from a system hyperparameter into a learnable per-step decision. This learnable

span–density interface enables task-adaptive frame acquisition: the model can retrieve dense frames for short, motion-sensitive events and sparse frames for long-range semantic understanding, acquiring multi-granularity evidence with a single retrieval step. This reduces reliance on repeated multi-round retrieval calls, which often introduce long inference contexts and complex tool-call training designs.

Furthermore, based on the explicit retrieval boundary created by this tokenized interface, we propose **Segment-Decoupled GRPO (SD-GRPO)**, which splits each rollout at the retrieval boundary and assigns role-specific token-level advantages, separately crediting the sampling decision and the answer reasoning. This provides targeted credit for temporal selection and sampling density while preserving the end-to-end answer signal. To train this behavior, we curate task-balanced **DM-CoT-74k** for supervised fine-tuning and **DM-RL-45k** for reinforcement learning, explicitly designed to cultivate robust native tokenized adaptive retrieval capabilities. Extensive experiments across six benchmarks spanning temporal grounding, grounded VideoQA, and long-form video understanding show that DynFrame-4B is competitive with strong 7B–8B baselines, while DynFrame-8B achieves state-of-the-art results on most metrics.

In summary, our contributions are three-fold:

- We introduce **DynFrame**, a multimodal reasoning framework that emits temporal span and sampling density as native tokens, turning adaptive temporal evidence acquisition from an externally scheduled tool operation into a model-native reasoning capability.
- We curate **DM-CoT-74k** for cold-start SFT and **DM-RL-45k** for reinforcement learning, and propose **SD-GRPO**, which uses the explicit retrieval boundary to assign role-specific token-level advantages to the sampling and reasoning segments.
- Across six benchmarks spanning temporal grounding, grounded VideoQA, and long-form video understanding, DynFrame-4B is competitive with strong 7B–8B baselines, while DynFrame-8B achieves state-of-the-art results on most metrics.

2 Related Work

Multimodal Chain-of-Thought for video reasoning. Multimodal chain-of-thought extends textual CoT [33] by allowing intermediate reasoning to interact with visual evidence rather than relying on a fixed visual pass. Early video reasoning and post-training methods, such as Video-R1 [6], VideoChat-R1 [20], VideoRFT [30], Temporal-RLT [19], improve multi-step video inference through supervised fine-tuning or reinforcement learning, but they mostly reason over the visual tokens supplied at the beginning of generation. A growing *thinking-with-video* line instead lets the model actively revisit visual evidence during inference. VITAL [41] and LongVT [36] formulate evidence acquisition as tool-based clip retrieval; LOVE-R1 [8] and VideoZoomer [5] use zoom-in or temporal focusing; VideoChat-R1.5 [35] performs iterative perception; Video-o3 [39], Open-o3 Video [24], and VideoTemp-o3 [21] explore native interleaved tool invocation. These methods show that active evidence acquisition is important for long-video reasoning. However, their retrieval granularity is still largely governed by external tools, preset zoom/spotlight modes, or system-defined visual-token budgets. As a result, obtaining the right amount of visual evidence for each question often depends on repeated retrieval calls, which expand the inference context and make training harder.

Frame sampling for video MLLMs. Frame sampling determines which visual evidence is available to the reasoner and directly affects both accuracy and efficiency. Uniform sampling at a fixed interval [23, 40, 15] is simple but content-agnostic, so it can miss short events in long videos. Modern video MLLMs [2, 1] provide dynamic-FPS or timestamp-aligned video interfaces, but the sampling rate is set by the calling pipeline rather than predicted by the model during reasoning. Query-conditioned selectors such as AKS [28], FOCUS [37], and Frame-Voyager [38] improve over uniform sampling by ranking frames according to query relevance, but they usually commit to a fixed frame set before reasoning begins. Agentic video systems lift this one-shot constraint by allowing inference-time retrieval, yet their visual budget is still largely controlled by system-level schedules, fixed per-call caps, slow/fast presets, or external visual-token quotas.

Reinforcement learning for MLLM reasoning. GRPO from DeepSeek-R1 [11, 26] has been adopted to post-train MLLMs for image VQA [42, 13], video reasoning [6, 29, 22], and tool-augmented generation [44, 41]. These formulations apply a single trajectory-level advantage to

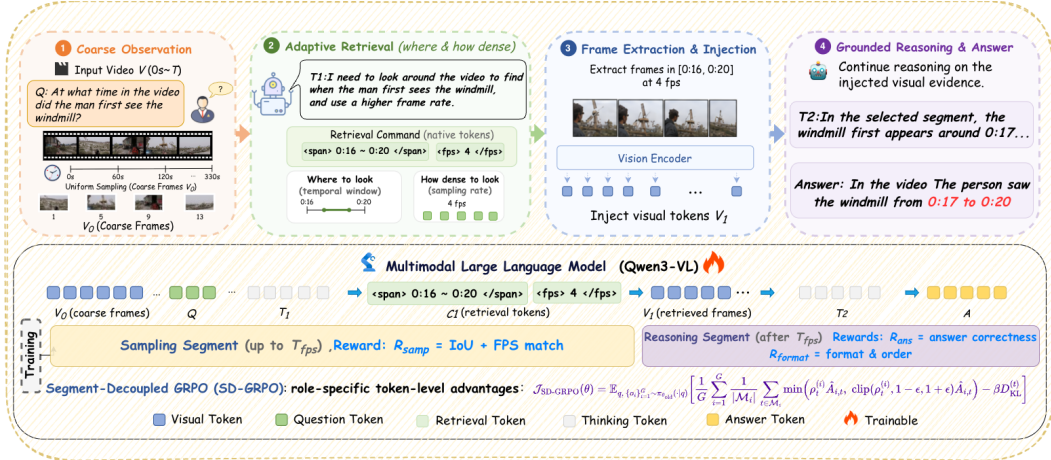


Figure 2: **Overview of DynFrame.** The model interleaves tokenized temporal retrieval ($\langle \text{span} \rangle$, $\langle \text{fps} \rangle$) with on-the-fly frame injection inside a single autoregressive pass. SD-GRPO splits each rollout at the retrieval boundary and applies segment-specific advantages so that the sampling decision and the answer reasoning are credited separately.

every token in the rollout, entangling the credit for committing a retrieval action with the credit for producing the final answer. Variants that decouple along task difficulty [41], multi-step vs. single-step turn [8], or reward component [36] still share one advantage across all tokens within a rollout, leaving the *where-to-look* decision without a dedicated training signal.

3 Method

We propose **DynFrame**, an end-to-end trainable video reasoning framework that unifies adaptive frame retrieval with dynamically interleaved vision-language reasoning within a single generative process (Fig. 2). Built upon Qwen3-VL [1], DynFrame introduces three key designs: (i) a *tokenized retrieval interface*, where the model specifies which temporal span and at what sampling density to retrieve by generating structured tokens; (ii) a *dynamic frame injection* mechanism that encodes the retrieved frames and inserts them into the decoding context on-the-fly; and (iii) *Segment-Decoupled GRPO*, which decouples rewards across response segments to separately optimize temporal selection and answer reasoning. We detail the dynamic multimodal CoT in §3.1, the two-stage training procedure in §3.2, and the dataset curation pipeline in §3.3.

3.1 Dynamic Multimodal Chain-of-Thought

3.1.1 Generation with Adaptive Frame Retrieval

Given a user question Q and an initial video observation V_0 (uniformly sampled frames), DynFrame generates a multimodal reasoning trajectory that interleaves textual reasoning with adaptive retrieval. In our main setting, this forms a three-stage process: *coarse reasoning* \rightarrow *retrieval* \rightarrow *grounded reasoning*. The model first produces an initial reasoning segment T_1 based on Q and a coarse understanding of V_0 , then generates a retrieval command C_1 to request additional evidence from the original video. After the retrieved frames V_1 are injected, the model continues reasoning over the augmented visual context and produces the final answer A . The trajectory is:

$$\mathbf{s} = \{V_0, T_1, C_1, V_1, T_2, A\}. \quad (1)$$

In this work, we instantiate a single retrieval round, which provides a favorable accuracy–cost trade-off on our benchmarks. The same tokenized interface can be extended to multiple rounds by emitting additional retrieval commands.

Tokenized retrieval interface. We design a set of special tokens to express video evidence acquisition as part of the model output. The model emits $\langle \text{span} \rangle t_s \text{--} t_e \langle / \text{span} \rangle$ to specify a temporal window and $\langle \text{fps} \rangle f \langle / \text{fps} \rangle$ to specify the sampling frame rate, which together parameterize the retrieval command C_1 . This turns frame selection from a fixed preprocessing choice into a learnable

decision within the autoregressive generation trajectory, enabling adaptive, multi-granularity temporal sampling conditioned on the current reasoning context. Predicting both the temporal window and the sampling rate is essential, as different queries demand different granularities: a brief hand gesture requires dense frames within a narrow window, whereas long-form narrative understanding may only need sparse keyframes.

3.1.2 Dynamic Frame Injection

We perform on-the-fly frame injection during autoregressive generation. The `</fps>` token closing a retrieval command acts as a retrieval trigger: the system parses the preceding `` and `<fps>` fields to obtain (t_s, t_e, f) and extracts

$$N = \lfloor (t_e - t_s) \times f \rfloor \quad (2)$$

frames uniformly distributed within $[t_s, t_e]$, capped by a maximum frame budget via uniform subsampling when necessary, and independent of the initial uniform sampling. Retrieved frames pass through the frozen vision encoder, and for each frame we emit a timestamped visual token subsequence containing its timestamp, vision boundary tokens, and $H'W'/m^2$ visual placeholder tokens, where H', W' are the post-encoder spatial dimensions and m is the patch merge size. The new visual tokens are appended to the generation buffer, yielding an extended sequence $\mathbf{x}' = [\mathbf{x}_{1:L}; \mathbf{v}_{1:N}]$. The decoder then re-prefills KV states over \mathbf{x}' before incremental decoding resumes:

$$\mathbf{H}_l = \text{SelfAttn}_l(\mathbf{x}'), \quad l = 1, \dots, L_{\text{dec}}, \quad (3)$$

so that the inserted frames can attend to all prior reasoning tokens and vice versa. This bidirectional attention lets the post-injection reasoning ground its claims directly on the retrieved frames rather than on a textual restatement of them.

3.2 Training Framework

Our training procedure consists of two stages: (1) cold-start supervised fine-tuning (SFT) to establish interleaved retrieval and reasoning behaviors, and (2) reinforcement learning via SD-GRPO to jointly improve temporal selection and grounded multimodal reasoning. We train on two curated multi-task datasets. **DM-CoT-74k** provides supervised trajectories with interleaved retrieval commands (span/FPS) and grounded reasoning. **DM-RL-45k** provides question–video pairs with ground-truth temporal spans, FPS targets, and answers, enabling reward computation for both sampling quality and answer correctness. Full dataset details are in §3.3.

3.2.1 Cold-Start Supervised Fine-Tuning

We bootstrap DynFrame with SFT on **DM-CoT-74k** by maximizing the likelihood of interleaved reasoning and retrieval tokens:

$$\mathcal{L}_{\text{SFT}} = -\frac{1}{|\mathcal{M}|} \sum_{t \in \mathcal{M}} \log p_{\theta}(x_t | x_{<t}), \quad (4)$$

where $\mathcal{M} = \{t : x_t \neq \langle \text{video_pad} \rangle\}$ denotes positions whose targets are not visual placeholder tokens. We exclude `<video_pad>` tokens within injected segments from the loss, as they correspond to vision features rather than predicted text. In contrast, we retain timestamp tokens and vision boundary tokens (e.g., `<vision_start>`, `<vision_end>`) as SFT targets, which encourages the model to learn temporal boundary prediction.

3.2.2 Segment-Decoupled GRPO

While SFT teaches the model to imitate interleaved retrieval–reasoning trajectories, we observe a *credit-assignment imbalance* when directly applying GRPO to our retrieval-augmented generation. On challenging questions, the model often predicts a reasonable span/FPS but still fails in post-injection reasoning, causing the negative outcome reward to penalize the retrieval tokens as well. Conversely, when the final answer can be obtained from coarse initial observations (e.g., shortcut cues), a positive outcome reward may incorrectly reinforce inaccurate span/FPS predictions. To address this, we propose **Segment-Decoupled GRPO (SD-GRPO)**, which separates optimization for the *sampling segment* (span/FPS tokens before injection) from the *grounded reasoning segment*

(tokens after injection). SD-GRPO assigns a retrieval-specific reward to the sampling segment and an answer-specific reward to the post-injection segment, improving credit assignment and stabilizing retrieval–reasoning co-adaptation.

We extend standard GRPO [26] rollouts to accommodate dynamic video insertion. Given a question Q and video V , we sample G completions $\{o_1, \dots, o_G\}$ from the current policy π_θ . When the model generates the retrieval terminator token $\langle /fps \rangle$ during a rollout, the system triggers dynamic frame injection and appends the corresponding visual token sequences to the generation buffer. We denote the position of $\langle /fps \rangle$ as T_{fps} , which partitions each completion into a *sampling segment* $o^{\text{samp}} = \{o_t\}_{t=1}^{T_{fps}}$ and a *reasoning segment* $o^{\text{reas}} = \{o_t\}_{t=T_{fps}+1}^T$. We define three reward signals.

(1) Sampling reward. The sampling reward R_{samp} evaluates the quality of the frame acquisition decision, combining temporal span overlap with a smooth FPS matching score:

$$R_{\text{samp}} = \lambda_1 \cdot \text{IoU}([\hat{t}_s, \hat{t}_e], [t_s^*, t_e^*]) + \lambda_2 \cdot \max\left(0, 1 - \frac{|\hat{f} - f^*|}{f_{\text{max}}}\right), \quad (5)$$

where $[\hat{t}_s, \hat{t}_e]$ and \hat{f} are the model’s predictions, $[t_s^*, t_e^*]$ and f^* are the ground-truth annotations, and the FPS term decays linearly from full credit at $\hat{f} = f^*$ to zero at deviations exceeding f_{max} . Both terms are bounded in $[0, 1]$, so we combine them at equal scale with $\lambda_1 = \lambda_2 = 0.5$. The two terms play asymmetric roles in practice: span IoU localizes *where* evidence lies and is the dominant supervisor, while the FPS term acts as a fine-grained corrector that selects density *within* an already-localized window. This is consistent with the intuition that any FPS choice is low-utility once the span is wrong, and is verified empirically in §4.3.

(2) Answer reward. The answer reward R_{ans} evaluates final-task correctness: we use exact match for multiple-choice VideoQA, and IoU for temporal grounding.

(3) Format reward. We additionally apply a rule-based format reward R_{format} to ensure the output follows the required structure (reasoning segment, span/FPS fields, and answer segment with correct ordering and pairing).

Token-Level Segment-Decoupled Advantage. The key idea of SD-GRPO is to assign advantages according to which segment a token belongs to, rather than using a single scalar advantage for the whole completion. For each group of G rollouts, we compute two group-normalized advantages:

$$\hat{A}_i^{\text{samp}} = \frac{R_{\text{samp},i} - \mu_{\text{samp}}}{\sigma_{\text{samp}} + \epsilon}, \quad \hat{A}_i^{\text{ans}} = \frac{(R_{\text{ans},i} + R_{\text{format},i}) - \mu_{\text{ans}}}{\sigma_{\text{ans}} + \epsilon}, \quad (6)$$

where μ and σ are computed within the group for each reward. We then assign per-token advantages by:

$$\hat{A}_{i,t} = \begin{cases} \hat{A}_i^{\text{samp}} + \hat{A}_i^{\text{ans}} & \text{if } t \leq T_{\text{fps}} \quad (\text{sampling segment}) \\ \hat{A}_i^{\text{ans}} & \text{if } t > T_{\text{fps}} \quad (\text{reasoning segment}). \end{cases} \quad (7)$$

Intuitively, tokens before $\langle /fps \rangle$ are directly responsible for span/FPS decisions and thus receive R_{samp} -based credit, while also receiving an end-to-end signal via R_{ans} . Tokens after $\langle /fps \rangle$ cannot change the already-committed sampling decision, and are optimized solely for answer correctness.

Optimization. With token-level segment-decoupled advantages, we optimize the SD-GRPO objective as follows:

$$\mathcal{J}_{\text{SD-GRPO}}(\theta) = \mathbb{E}_{q, \{o_i\}_{i=1}^G \sim \pi_{\theta_{\text{old}}}(\cdot|q)} \left[\frac{1}{G} \sum_{i=1}^G \frac{1}{|\mathcal{M}_i|} \sum_{t \in \mathcal{M}_i} \min(\rho_t^{(i)} \hat{A}_{i,t}, \text{clip}(\rho_t^{(i)}, 1-\epsilon, 1+\epsilon) \hat{A}_{i,t}) - \beta D_{\text{KL}}^{(t)} \right], \quad (8)$$

where $q = \{Q, V\}$ denotes the input question and video, and $\{o_i\}_{i=1}^G$ are G rollouts sampled from the behavior policy $\pi_{\theta_{\text{old}}}$. $\mathcal{M}_i = \{t : o_{i,t} \notin \mathcal{V}_{\text{pad}}\}$ excludes visual placeholder tokens (e.g., $\langle \text{video_pad} \rangle$) from optimization. The importance ratio is $\rho_t^{(i)} = \pi_\theta(o_{i,t} | q, o_{i,<t}) / \pi_{\theta_{\text{old}}}(o_{i,t} | q, o_{i,<t})$, and $D_{\text{KL}}^{(t)}$ is the per-token KL divergence against the reference policy π_{ref} with coefficient β . Compared to the standard GRPO that uses a single trajectory-level advantage for all tokens, SD-GRPO assigns segment-dependent token-level advantages $\hat{A}_{i,t}$, enabling targeted optimization for both *where to look* (sampling segment) and *how to reason* (reasoning segment).

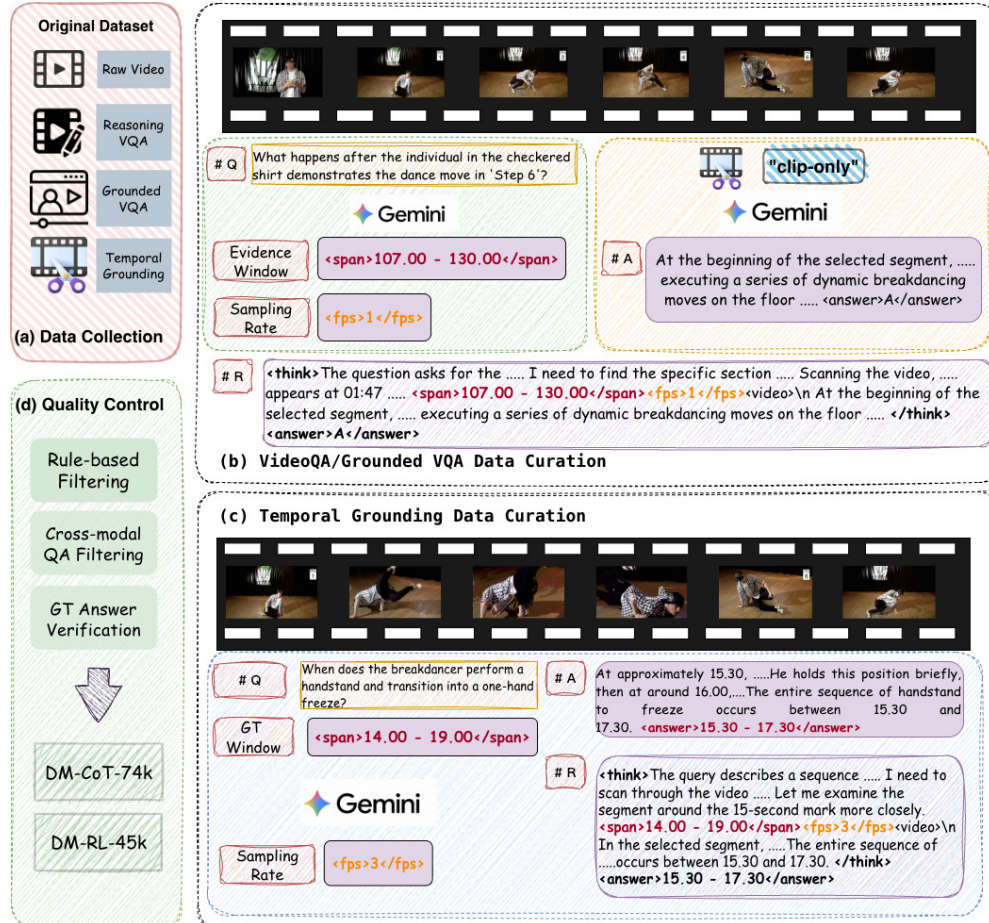


Figure 3: **Data curation pipeline for DM-CoT-74k and DM-RL-45k.** (a) Sources: VideoQA, grounded VideoQA, and temporal grounding benchmarks. (b) For VideoQA without temporal annotations, Gemini selects the evidence window and sampling rate, then answers under a “clip-only” constraint enforced at the prompt level. (c) For temporal grounding, ground-truth windows are reused; Gemini only selects an activity-adaptive FPS. (d) Rule-based and answer-consistency filters yield the final mixtures.

3.3 Training Data Curation

Training DynFrame requires trajectories that interleave textual reasoning with span+FPS retrieval commands and grounded answers. Since no public dataset provides this format, we curate two task-balanced mixtures over temporal grounding, VideoQA, and grounded VideoQA, sourced from Charades-STA [27], ActivityNet-MR [17], Video-R1 [6], ReXTime [3], and NEX-T-GQA [34]. All samples are converted into the unified retrieval-augmented format of §3.1.1.

For VideoQA and grounded VideoQA, where temporal annotations are absent, we prompt Gemini-3-Pro [10] to identify the relevant evidence window, propose an FPS, and produce the answer under the constraint that it “only rewatched the proposed window”—enforced at the prompt level rather than by re-uploading trimmed clips, which keeps construction cost low. For temporal grounding, the human-annotated boundary is reused verbatim with a 0.5–2 s random margin to provide context, and Gemini is queried only for an activity-adaptive FPS conditioned on the span. Because no public video dataset provides per-segment FPS supervision, the FPS targets used during RL are inherited from this teacher; the temporal IoU term in R_{samp} remains anchored to human-annotated boundaries, which is consistent with our design of treating IoU as the dominant supervisory signal.

We then apply two filtering stages: rule-based checks discard samples with missing or reversed retrieval fields, and an answer-consistency check drops teacher answers that disagree with the ground-truth label. Together they remove roughly 40% of raw teacher outputs. The final 74k SFT mixture

comprises $\sim 30\%$ temporal grounding, $\sim 45\%$ VideoQA, and $\sim 25\%$ grounded VideoQA; DM-RL-45k follows a similar ratio. Detailed prompts used for data generation are provided in Appendix A.

4 Experiments

4.1 Experimental Setup

Benchmarks. We evaluate on six benchmarks spanning three task families: (i) *grounded VideoQA*—NExT-GQA [34], with answer accuracy (Acc) and grounding mIoU; (ii) *temporal sentence grounding*—Charades-STA [9] and ActivityNet-MR [17], with $R@\{0.3, 0.5, 0.7\}$ and mIoU; (iii) *long-form video understanding*—Video-MME (w/o sub.) [7], MLVU (M-Avg) [45], and LVBench [31], all measured by multi-choice accuracy.

Implementation. We build DynFrame on Qwen3-VL-Thinking at 4B and 8B with the visual encoder frozen. The initial pass uniformly samples at $f_1=2$ fps, and the adaptive retrieval round uses a model-predicted $f_2 \in [1, 6]$ fps, with up to $N=128$ frames retrieved. SFT runs 4,000 steps at $\text{lr } 1 \times 10^{-5}$, batch 256, on 64 H200 GPUs (AdamW); RL with SD-GRPO uses $\text{lr } 1 \times 10^{-6}$, group $G=8$, temperature 1.0, for 1,000 further steps. Detailed inference-cost comparisons across benchmarks and methods are provided in Appendix C.

Table 1: **Comparison of our method with existing methods across six benchmarks.** “–” indicates the original paper does not evaluate on that benchmark, or the model’s output format is incompatible with the metric.

Model	Size	NExT-GQA		Charades-STA				ActivityNet-MR				V-MME	MLVU	LVB
		Acc	mIoU	R@.3	R@.5	R@.7	mIoU	R@.3	R@.5	R@.7	mIoU	w/o sub	M-Avg	Acc
<i>General / Single-turn Video MLLMs</i>														
Qwen2.5-VL [2]	7B	76.5	30.5	64.7	43.1	22.8	43.6	41.6	23.2	9.5	28.9	65.1	70.2	45.3
InternVL3 [46]	8B	80.4	30.0	–	–	–	–	–	–	–	–	66.3	71.4	47.0
Qwen3-VL (Thinking) [1]	4B	73.8	33.4	80.5	69.2	44.6	59.0	49.8	30.4	14.1	34.5	68.9	75.7	53.5
Qwen3-VL (Thinking) [1]	8B	75.4	35.1	81.6	70.8	45.8	59.9	51.8	32.4	15.6	36.2	71.8	75.1	55.8
Video-R1-7B [6]	7B	77.3	–	63.5	44.0	22.5	43.8	40.0	22.5	9.5	28.5	61.4	–	–
<i>Thinking-with-Video / Tool-Augmented Methods</i>														
Temporal-RLT [19]	7B	78.7	37.3	79.6	67.9	44.1	57.0	56.9	38.4	20.2	39.0	57.6	–	–
VITAL [41]	7B	78.7	43.0	83.1	72.0	46.7	59.9	70.9	50.8	31.6	49.8	64.1	–	–
LongVT [36]	7B	70.4	17.4	41.0	25.8	11.7	27.2	32.4	18.6	9.2	20.5	–	–	41.3
VideoZoomer [5]	7B	–	–	–	–	–	–	–	–	–	–	65.2	68.8	41.5
LOVE-R1 [8]	7B	73.0	30.5	74.0	41.0	14.0	44.8	49.0	24.0	13.0	30.4	66.2	67.4	48.2
VideoChat-R1.5 [35]	7B	79.9	–	82.8	71.6	48.3	60.6	52.4	32.3	16.8	35.5	67.1	70.9	48.4
Video-o3 [39]	7B	–	–	83.3	71.9	49.0	60.7	–	–	–	–	66.5	72.1	47.6
DynFrame-4B (ours)	4B	77.6	41.5	83.5	71.0	46.5	60.0	70.4	49.2	28.6	47.5	69.5	76.3	54.8
DynFrame-8B (ours)	8B	80.0	44.3	85.1	72.5	49.4	61.7	72.4	52.0	33.1	51.5	72.3	77.1	56.9

4.2 Comparison with State-of-the-Art

Temporal sentence grounding. On Charades-STA, DynFrame-8B reaches a new state of the art at 61.7 mIoU, surpassing the previous best thinking-with-video method Video-o3 (60.7); the 4B variant remains competitive at 60.0 mIoU, matching VITAL-7B (59.9) at half the parameter count. On the more challenging ActivityNet-MR, DynFrame-8B improves over the strongest baseline VITAL-7B by +1.7 mIoU. These gains show that a single round of joint span–density retrieval can match or surpass multi-round tool-call methods, with larger advantages on longer videos.

Grounded VideoQA. On NExT-GQA, DynFrame-8B achieves the best joint score among grounding-capable models (80.0 Acc / 44.3 mIoU), improving over VITAL-7B by +1.3 on both metrics and over its Qwen3-VL-Thinking-8B backbone by +4.6 Acc / +9.2 mIoU. Although InternVL3-8B reports a slightly higher accuracy (80.4), its 30.0 mIoU shows that the correct answers are not visually grounded. The simultaneous improvement on both metrics confirms that SD-GRPO effectively credits the sampling decision and the answer-reasoning segment separately.

Long-form video understanding. On Video-MME / MLVU / LVBench, DynFrame-8B sets new best results across all three long-form benchmarks (72.3/77.1/56.9), improving over its strong Qwen3-VL-Thinking-8B backbone by +0.5/+2.0/+1.1. The 4B variant also surpasses every 7B tool-augmented method (LOVE-R1, VideoChat-R1.5, Video-o3) on long-form video. Together

with the grounding and grounded-VideoQA results, these findings show that learnable span-density retrieval brings complementary gains across short-form grounding, grounded VideoQA, and long-form video understanding.

4.3 Ablation Study

Table 2: **Ablation studies on the 8B model.** NEX-T-GQA and Charades-STA report mIoU; V-MME and LVBench report accuracy. Shaded rows are our default. (a) Masking strategy for injected frames. (b) Effectiveness of SD-GRPO. (c) Robustness to the initial sampling rate f_1 . (d) Effectiveness of dynamic retrieval FPS f_2 .

Variant	N-GQA	Cha	V-MME	LVB
Mask all video tokens	18.1	26.4	36.3	39.4
Mask video pad only	44.3	61.7	72.3	56.9

Variant	N-GQA	Cha	V-MME	LVB
SFT only	41.5	58.7	70.0	54.5
+ vanilla GRPO	42.2	59.5	70.3	54.8
+ SD-GRPO	44.3	61.7	72.3	56.9

Variant	N-GQA	Cha	V-MME	LVB
Qwen3-VL, $f_1=0.5$	23.7	46.3	58.2	45.0
Qwen3-VL, $f_1=2$	35.1	59.9	71.8	55.8
DynFrame, $f_1=0.5, f_2=dyn$	42.5	60.5	70.5	55.1
DynFrame, $f_1=2, f_2=dyn$	44.3	61.7	72.3	56.9

Variant	N-GQA	Cha	V-MME	LVB
DynFrame, $f_2=2$ fixed	41.9	58.9	70.2	55.8
DynFrame, $f_2=dyn$	44.3	61.7	72.3	56.9

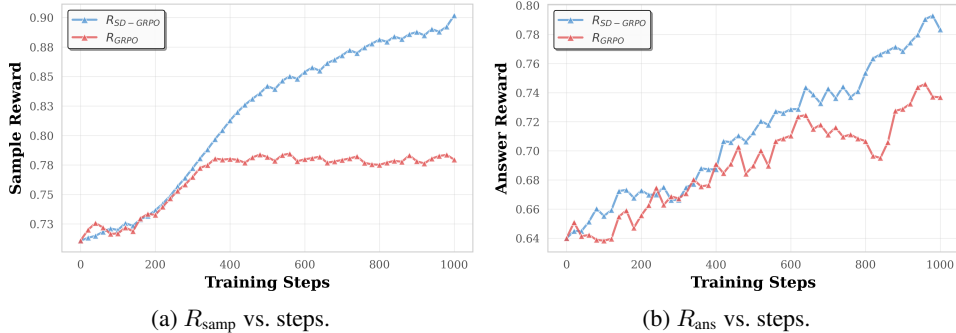


Figure 4: **Reward dynamics during RL.** SD-GRPO lifts both the sampling reward R_{samp} and the answer reward R_{ans} over vanilla GRPO.

(a) Masking strategy. During SFT, only the visual placeholder tokens (`<|video_pad|>`) are excluded from the loss because they encode raw vision features rather than predicted text, while timestamps and vision-boundary markers (`<|vision_start|>`, `<|vision_end|>`) are kept as supervision targets. Masking these additional tokens causes a sharp drop in performance, confirming that they act as anchors that align the injected frames with the reasoning context. **(b) SD-GRPO.** Building on this SFT initialization, we next examine the effect of segment-decoupled RL. SFT \rightarrow vanilla GRPO \rightarrow SD-GRPO improves metrics monotonically (Charades mIoU 58.7 \rightarrow 59.5 \rightarrow 61.7), with SD-GRPO consistently outperforming vanilla GRPO across all four benchmarks. Fig. 4 further shows that SD-GRPO yields higher sampling and answer rewards throughout training, confirming that segment-level credit assignment effectively decouples the sampling decision from the answer reasoning. **(c) Robustness to f_1 .** Beyond training-time choices, we also study how the model behaves under tighter initial frame budgets. Reducing f_1 from 2 to 0.5 fps causes the Qwen3-VL-Thinking-8B backbone to degrade substantially, with drops of up to 13.6 points across the four benchmarks. In contrast, DynFrame degrades by at most 1.8 points, suggesting that dynamic retrieval can recover most of the evidence missed by a sparse initial pass. **(d) Dynamic FPS.** Finally, we verify the necessity of letting the model choose its retrieval frame rate. Replacing the model-predicted f_2 with a fixed 2 fps rate consistently reduces performance by 1.1–2.8 points across all four benchmarks, confirming that DynFrame can adaptively select different sampling densities for different questions, acquiring evidence at the appropriate granularity. Detailed analysis of predicted spans and FPS is provided in Appendix B.

5 Conclusion

We presented DynFrame, a dynamic multimodal reasoning framework that turns visual evidence acquisition into a model-native decision. By predicting both the temporal window and the sampling density, DynFrame jointly decides where to retrieve and how densely to sample, acquiring task-adaptive, multi-granularity evidence with a single retrieval step. To train this behavior, we curated DM-CoT-74k and DM-RL-45k, and introduced Segment-Decoupled GRPO, which separately credits the sampling decision and the answer reasoning. Experiments across grounded VideoQA, temporal grounding, and long-form video understanding show that DynFrame-4B is competitive with strong 7B–8B baselines, while DynFrame-8B achieves new best results on most metrics.

References

- [1] Shuai Bai, Keqin Chen, Wenbin Ge, Xuejing Liu, Jialin Wang, Sibao Song, Kai Dang, Shijie Wang, Peng Wang, Jun Tang, et al. Qwen3-vl: Advancing multimodal perception across arbitrarily-resolution visual inputs. *arXiv preprint arXiv:2511.21631*, 2025.
- [2] Shuai Bai, Keqin Chen, Xuejing Liu, Jialin Wang, Wenbin Ge, Sibao Song, Kai Dang, Peng Wang, Shijie Wang, Jun Tang, et al. Qwen2.5-vl technical report. *arXiv preprint arXiv:2502.13923*, 2025.
- [3] Jr-Jen Chen, Yu-Chien Liao, Hsi-Che Lin, Yu-Chu Yu, Yen-Chun Chen, and Yu-Chiang Frank Wang. Rextime: A benchmark suite for reasoning-across-time in videos. *arXiv preprint arXiv:2406.19392*, 2024.
- [4] Gheorghe Comanici, Eric Bieber, Mike Schaekermann, Ice Pasupat, Noveen Sachdeva, Inderjit Dhillon, et al. Gemini 2.5: Pushing the frontier with advanced reasoning, multimodality, long context, and next generation agentic capabilities, 2025. URL <https://arxiv.org/abs/2507.06261>.
- [5] Yang Ding, Yizhen Zhang, Xin Lai, Ruihang Chu, and Yujiu Yang. Videozoomer: Reinforcement-learned temporal focusing for long video reasoning. *arXiv preprint arXiv:2512.22315*, 2025. URL <https://arxiv.org/abs/2512.22315>.
- [6] Kaituo Feng, Kaixiong Gong, Bohao Li, Zonghao Guo, Yibing Wang, Tianshuo Peng, Junfei Wu, Xiaoying Zhang, Benyou Wang, and Xiangyu Yue. Video-r1: Reinforcing video reasoning in mllms. *arXiv preprint arXiv:2503.21776*, 2025.
- [7] Chaoyou Fu, Yuhan Dai, Yongdong Luo, Lei Li, Shuhuai Ren, Renrui Zhang, Zihan Wang, Chenyu Zhou, Yunhang Shen, Mengdan Zhang, et al. Video-mme: The first-ever comprehensive evaluation benchmark of multi-modal llms in video analysis. In *Proceedings of the IEEE/CVF Conference on Computer Vision and Pattern Recognition*, pages 24108–24118, 2025.
- [8] Shenghao Fu, Qize Yang, Yuan-Ming Li, Xihan Wei, Xiaohua Xie, and Wei-Shi Zheng. Love-r1: Advancing long video understanding with an adaptive zoom-in mechanism via multi-step reasoning. *arXiv preprint arXiv:2509.24786*, 2025.
- [9] Jiyang Gao, Chen Sun, Zhenheng Yang, and Ram Nevatia. Tall: Temporal activity localization via language query. In *Proceedings of the IEEE International Conference on Computer Vision*, pages 5267–5275, 2017.
- [10] Google DeepMind. Gemini 3 Pro Model Card. <https://deepmind.google/models/model-cards/gemini-3-pro>, May 2026. Model release: November 2025; last updated: May 2026. Accessed: 2026-05-25.
- [11] Daya Guo, Dejian Yang, Haowei Zhang, Junxiao Song, Ruoyu Zhang, Runxin Xu, Qihao Zhu, Shirong Ma, Peiyi Wang, Xiao Bi, et al. Deepseek-r1: Incentivizing reasoning capability in llms via reinforcement learning. *arXiv preprint arXiv:2501.12948*, 2025.
- [12] Zefeng He, Xiaoye Qu, Yafu Li, Siyuan Huang, Daizong Liu, and Yu Cheng. Framethinker: Learning to think with long videos via multi-turn frame spotlighting. *arXiv preprint arXiv:2509.24304*, 2025. To appear in ICLR 2026.
- [13] Wenbo Huang, Bingyi Jia, Zhenbang Zhai, et al. Vision-r1: Incentivizing reasoning capability in multimodal large language models. *arXiv preprint arXiv:2503.06749*, 2025.
- [14] Aaron Hurst, Adam Lerer, Adam P Goucher, Adam Perelman, Aditya Ramesh, Aidan Clark, AJ Ostrow, Akila Welihinda, Alan Hayes, Alec Radford, et al. Gpt-4o system card. *arXiv preprint arXiv:2410.21276*, 2024.
- [15] Peng Jin, Ryuichi Takanobu, Wancai Zhang, Xiaochun Cao, and Li Yuan. Chat-univi: Unified visual representation empowers large language models with image and video understanding. In *Proceedings of the IEEE/CVF Conference on Computer Vision and Pattern Recognition*, 2024.
- [16] Kimi Team, Angang Du, Bohong Yin, Bowei Xing, Bowen Qu, Bowen Wang, Cheng Chen, Chenlin Zhang, Chenzhuang Du, Chu Wei, et al. Kimi-vl technical report. *arXiv preprint arXiv:2504.07491*, 2025.
- [17] Ranjay Krishna, Kenji Hata, Frederic Ren, Li Fei-Fei, and Juan Carlos Niebles. Dense-captioning events in videos. In *Proceedings of the IEEE International Conference on Computer Vision*, pages 706–715, 2017.
- [18] Bo Li, Yuanhan Zhang, Dong Guo, Renrui Zhang, Feng Li, Hao Zhang, Kaichen Zhang, Peiyuan Zhang, Yanwei Li, Ziwei Liu, et al. Llava-onevision: Easy visual task transfer. *arXiv preprint arXiv:2408.03326*, 2024.

- [19] Hongyu Li, Songhao Han, Yue Liao, Junfeng Luo, Jialin Gao, Shuicheng Yan, and Si Liu. Reinforcement learning tuning for videollms: Reward design and data efficiency. *arXiv preprint arXiv:2506.01908*, 2025. URL <https://arxiv.org/abs/2506.01908>.
- [20] Xinhao Li, Ziang Yan, Desen Meng, Lu Dong, Xiangyu Zeng, Yinan He, Yali Wang, Yu Qiao, Yi Wang, and Limin Wang. Videochat-r1: Enhancing spatio-temporal perception via reinforcement fine-tuning. *arXiv preprint arXiv:2504.06958*, 2025.
- [21] Wenqi Liu, Yunxiao Wang, Shijie Ma, Meng Liu, Qile Su, Tianke Zhang, Haonan Fan, Changyi Liu, Kaiyu Jiang, Jiankang Chen, Kaiyu Tang, Bin Wen, Fan Yang, Tingting Gao, Han Li, Yinwei Wei, and Xuemeng Song. VideoTemp-o3: Harmonizing temporal grounding and video understanding in agentic thinking-with-videos. *arXiv preprint arXiv:2602.07801*, 2026. URL <https://arxiv.org/abs/2602.07801>.
- [22] Zuyan Liu et al. Video-rts: Rethinking reinforcement learning and test-time scaling for efficient and enhanced video reasoning. *arXiv preprint arXiv:2507.06485*, 2025.
- [23] Muhammad Maaz, Hanoona Rasheed, Salman Khan, and Fahad Shahbaz Khan. Video-chatgpt: Towards detailed video understanding via large vision and language models. *arXiv preprint arXiv:2306.05424*, 2023.
- [24] Jiahao Meng, Xiangtai Li, Haochen Wang, Yue Tan, Tao Zhang, Lingdong Kong, Yunhai Tong, Anran Wang, Zhiyang Teng, Yujing Wang, and Zhuochen Wang. Open-o3 Video: Grounded video reasoning with explicit spatio-temporal evidence. *arXiv preprint arXiv:2510.20579*, 2025. URL <https://arxiv.org/abs/2510.20579>.
- [25] Hao Shao, Shengju Qian, Han Xiao, Guanglu Song, Zhi Zong, Letian Wang, Yu Liu, and Hongsheng Li. Visual cot: Advancing multi-modal language models with a comprehensive dataset and benchmark for chain-of-thought reasoning. In *The Thirty-eighth Conference on Neural Information Processing Systems Datasets and Benchmarks Track*, 2024.
- [26] Zhihong Shao, Peiyi Wang, Qihao Zhu, et al. Deepseekmath: Pushing the limits of mathematical reasoning in open language models. *arXiv preprint arXiv:2402.03300*, 2024.
- [27] Young Chol Song. Temporal grounding of activities using multimodal large language models. *arXiv preprint arXiv:2407.06157*, 2024. URL <https://arxiv.org/abs/2407.06157>.
- [28] Xi Tang, Jihao Qiu, Lingxi Xie, Yunjie Tian, Jianbin Jiao, and Qixiang Ye. Adaptive keyframe sampling for long video understanding. In *Proceedings of the IEEE/CVF Conference on Computer Vision and Pattern Recognition*, 2025.
- [29] GRPO-CARE Team. Grpo-care: Consistency-aware reinforcement learning for video mllms. *arXiv preprint arXiv:2506.16141*, 2025.
- [30] Qi Wang, Yanrui Yu, Ye Yuan, Rui Mao, and Tianfei Zhou. Videortf: Incentivizing video reasoning capability in mllms via reinforced fine-tuning. *arXiv preprint arXiv:2505.12434*, 2025.
- [31] Weihao Wang, Zehai He, Wenyi Hong, Yean Cheng, Xiaohan Zhang, Ji Qi, Xiaotao Gu, Shiyu Huang, Bin Xu, Yuxiao Dong, Ming Ding, and Jie Tang. LVBench: An extreme long video understanding benchmark. *arXiv preprint arXiv:2406.08035*, 2024.
- [32] Yaoting Wang, Shengqiong Wu, Yuecheng Zhang, Shuicheng Yan, Ziwei Liu, Jiebo Luo, and Hao Fei. Multimodal chain-of-thought reasoning: A comprehensive survey. *arXiv preprint arXiv:2503.12605*, 2025.
- [33] Jason Wei, Xuezhi Wang, Dale Schuurmans, Maarten Bosma, Brian Ichter, Fei Xia, Ed Chi, Quoc Le, and Denny Zhou. Chain-of-thought prompting elicits reasoning in large language models. *Advances in Neural Information Processing Systems*, 35:24824–24837, 2022.
- [34] Junbin Xiao, Angela Yao, Yicong Li, and Tat-Seng Chua. Can I trust your answer? Visually grounded video question answering. In *Proceedings of the IEEE/CVF Conference on Computer Vision and Pattern Recognition (CVPR)*, pages 13204–13214, 2024.
- [35] Ziang Yan, Xinhao Li, Desen Meng, Lu Dong, Xiangyu Zeng, Yinan He, Yali Wang, Yu Qiao, Yi Wang, and Limin Wang. Videochat-r1.5: Visual test-time scaling to reinforce multimodal reasoning by iterative perception. In *Advances in Neural Information Processing Systems (NeurIPS)*, 2025.
- [36] Zuhao Yang, Sudong Wang, Kaichen Zhang, Keming Wu, Sicong Leng, Yifan Zhang, Bo Li, Chengwei Qin, Shijian Lu, Xingxuan Li, and Lidong Bing. Longvt: Incentivizing “thinking with long videos” via native tool calling. *arXiv preprint arXiv:2511.20785*, 2025. To appear in CVPR 2026.

- [37] Huanjin Yao et al. Focus: Efficient keyframe selection for long video understanding. *arXiv preprint arXiv:2510.27280*, 2025.
- [38] Shoubin Yu, Jaemin Cho, Prateek Yadav, and Mohit Bansal. Frame-voyager: Learning to query frames for video large language models. In *Advances in Neural Information Processing Systems*, 2024.
- [39] Xiangyu Zeng, Zhiqiu Zhang, Yuhan Zhu, Xinhao Li, Zikang Wang, Changlian Ma, Qingyu Zhang, Zizheng Huang, Kun Ouyang, et al. Video-o3: Native interleaved clue seeking for long video multi-hop reasoning. *arXiv preprint arXiv:2601.23224*, 2026.
- [40] Hang Zhang, Xin Li, and Lidong Bing. Video-llama: An instruction-tuned audio-visual language model for video understanding. In *Proceedings of the 2023 Conference on Empirical Methods in Natural Language Processing*, 2023.
- [41] Haoji Zhang, Xin Gu, Jiawei Liu, Mingyang Li, Quan Wang, Zhibo Yang, Hongqing Yang, and Yansong Tang. Thinking with videos: Multimodal tool-augmented reinforcement learning for long video reasoning. *arXiv preprint arXiv:2508.04416*, 2025. To appear in CVPR 2026.
- [42] Kaituo Zhang et al. R1-vl: Learning to reason with multimodal large language models via reinforcement learning. *arXiv preprint arXiv:2503.12937*, 2025.
- [43] Yuanhan Zhang, Bo Li, Haotian Liu, Yong Jae Lee, Liangke Gui, Di Fu, Jiashi Feng, Ziwei Liu, and Chunyuan Li. Video instruction tuning with synthetic data. *arXiv preprint arXiv:2410.02713*, 2024.
- [44] Ziwei Zheng, Michael Yang, Jack Hong, Chenxiao Zhao, Guohai Xu, Le Yang, Chao Shen, and Xing Yu. Deepeyes: Incentivizing “thinking with images” via reinforcement learning. *arXiv preprint arXiv:2505.14362*, 2025.
- [45] Junjie Zhou, Yan Shu, Bo Zhao, Boya Wu, Shitao Xiao, Xi Yang, Yongping Xiong, Bo Zhang, Tiejun Huang, and Zheng Liu. MLVU: A comprehensive benchmark for multi-task long video understanding. *arXiv preprint arXiv:2406.04264*, 2024.
- [46] Jinguo Zhu, Weiyun Wang, Zhe Chen, Zhaoyang Liu, Shenglong Ye, Lixin Gu, Yuchen Duan, Hao Tian, Weijie Su, Jie Shao, et al. Internv13: Exploring advanced training and test-time recipes for open-source multimodal models. *arXiv preprint arXiv:2504.10479*, 2025.

Supplementary Material

A Data Generation Prompts

We provide the complete prompts used to query Gemini-3-Pro [4] for constructing our training data. We design two complementary prompts tailored to the annotation characteristics of each task type. For VideoQA and Grounded VQA, where only question–answer pairs are available without temporal annotations, we query Gemini to produce both temporal localization and answer reasoning from scratch. For temporal grounding, where ground-truth temporal boundaries already exist, we adopt a reformulative strategy by prompting Gemini to expand, clean, and canonicalize existing reasoning traces while preserving the original annotations. Both prompts share a unified adaptive FPS selection guideline to ensure consistent, content-aware sampling across the training mixture.

A.1 VideoQA & Grounded VQA Prompt

The prompt in Figure A1 performs two-stage annotation in a single API call via a structured JSON with two fields. In `zoom_in_cot`, the model reasons about which temporal segment contains the required visual evidence and concludes with `<time_span>` and `<fps>` tags, without predicting or guessing the answer. In `answer_cot`, the model assumes it has watched **only** that segment at the specified FPS and reasons step by step to produce the final answer. A three-tier FPS guideline (1–2 fps for static scenes, 3–4 fps for moderate dynamics, 5–6 fps for rapid actions) is embedded to ensure activity-adaptive sampling density.

A.2 Temporal Grounding Prompt

The prompt in Figure A2 reformulates existing reasoning traces rather than annotating from scratch. Given a trace with ground-truth temporal boundaries, the model expands the span by a random margin of 0.5–2.0 s on each side for contextual retrieval, relocates the expanded `<time_span>` and an adaptive `<fps>` tag to the front of the chain, and removes redundant temporal descriptions. The original unexpanded boundaries serve as the supervision signal.

Prompt for VideoQA & Grounded VQA Data Generation

System Prompt: You are a video analysis assistant. Answer based solely on the visual content of the video. Rely strictly on visual cues; ignore audio. Respond in valid, raw JSON only.

.....
User Prompt:

You will respond in valid, raw JSON with exactly two top-level keys.

JSON Structure:

```
{
  "zoom_in_cot": "Your step-by-step reasoning for selecting
the specific video segment. This string MUST end strictly
with the time span and FPS tags in the format
<span>START - END</span> <fps>N</fps>.",
  "answer_cot": "Your step-by-step reasoning after 'watching'
the selected segment. This string MUST end strictly with
the final answer wrapped in
<answer>OPTION_LETTER</answer>."
}
```

Workflow

1. Read the user's question and infer the precise visual evidence required.
2. Describe, step by step, how you would locate the segment that likely contains this evidence. Explain why this portion is critical.
3. Based on the nature and speed of the target activity, recommend an appropriate FPS for analysis.
4. Conclude your "zoom_in_cot" reasoning by appending the time span and FPS tags. **Do NOT** provide or guess the answer in this field.
5. After that, imagine you have now watched **ONLY** that segment at the specified FPS. Using the visual information in the segment, reason step-by-step to reach the answer.
6. This reasoning plus the final answer (wrapped in `<answer></answer>`) goes into "answer_cot".

FPS Selection Guideline

- **1–2 fps:** Static or quasi-static scenes with minimal temporal variation (e.g., reading text/signs, appearance attributes, object identification, colors, a person standing still).
- **3–4 fps:** Moderately dynamic scenarios with clear temporal progression (e.g., general activities, object interactions, walking, cooking step-by-step, gesture recognition, conversations).
- **5–6 fps:** Rapid, fine-grained actions requiring frame-by-frame analysis (e.g., fast actions, rapid motion, counting quick events, sports movements, catching/throwing a ball).

Strict Rules

- Output must be raw JSON only (no markdown fences like ```` json`).
- Time span must use seconds with two decimal places (e.g., 5.00 - 9.00).
- The "zoom_in_cot" value must end with the closing tag `</fps>`. Do not add any punctuation, whitespace, or words after this tag.
- The final answer must appear only once, inside `<answer></answer>`, at the very end of "answer_cot".
- Inside `<answer></answer>`, output only the letter A, B, C, D... (do not include the option text).
- FPS must be an integer between 1 and 6.

Question: {question}

Options: {options}

Figure A1: **Data generation prompt for VideoQA.** We prompt Gemini-3-Pro to jointly perform temporal evidence identification with adaptive FPS recommendation and clip-constrained answer generation in a single call via two structured JSON fields. The FPS selection guideline ensures the sampling rate matches the visual dynamics of the target activity.

Prompt for Temporal Grounding Data Generation

System Prompt: You are a video analysis assistant specializing in temporal grounding. Respond in valid, raw text only following the exact output format specified below.

User Prompt:
 You are given a temporal grounding reasoning trace that contains a thinking process and an answer. Your task is to **reformulate** it into our canonical format, **expand the temporal window for contextual evidence**, and **recommend an appropriate FPS** for the identified temporal span. Perform the following operations:

Workflow

- Starting from the original temporal span in the input, expand the start and end boundaries by a random margin of 0.5–2.0 seconds on each side to provide additional temporal context.
- Move the expanded temporal span to the front of the thinking process, formatted as `START - END` (seconds with two decimal places, e.g., `29.50 - 74.00`).
- Remove redundant or repeated temporal descriptions in the thinking process. Keep the reasoning concise and non-repetitive.
- Based on the duration of the **expanded span** and the nature of the activity described, append an FPS tag `<fps>N</fps>` immediately after the `` tag.
- Extract only the **original** start and end timestamps as the final answer (e.g., `30.00 - 72.00`).

FPS Selection Guideline

- 1–2 fps:** Static or quasi-static scenes with minimal temporal variation (e.g., reading text/signs, appearance attributes, object identification, colors, a person standing still).
- 3–4 fps:** Moderately dynamic scenarios with clear temporal progression (e.g., general activities, object interactions, walking, cooking step-by-step, gesture recognition, conversations).
- 5–6 fps:** Rapid, fine-grained actions requiring frame-by-frame analysis (e.g., fast actions, rapid motion, counting quick events, sports movements, catching/throwing a ball).

Output Format

```

<think>
<span>EXPANDED_START - EXPANDED_END</span> <fps>N</fps>
[Rest of the cleaned reasoning...]
</think>
<answer>ORIGINAL_START - ORIGINAL_END</answer>
  
```

Strict Rules

- Inside `<think>`, the first line must be `<time_span>EXPANDED_START - EXPANDED_END</time_span> <fps>N</fps>`.
- FPS must be an integer between 1 and 6.
- The `<time_span>` must contain the expanded temporal span.
- The `<answer>` must contain only the original, unexpanded start and end timestamps, with no additional text.
- Remove redundant temporal descriptions but preserve the core reasoning logic.

Input: {current_input}
Output:

Figure A2: **Data reformulation and FPS annotation prompt for temporal grounding.** Given an existing reasoning trace with ground-truth temporal boundaries, we prompt Gemini-3-Pro to canonicalize the format by expanding the temporal window for contextual evidence, relocating the contextual span to the front, cleaning redundant descriptions, recommending an activity-adaptive FPS, and extracting the original minimal answer.

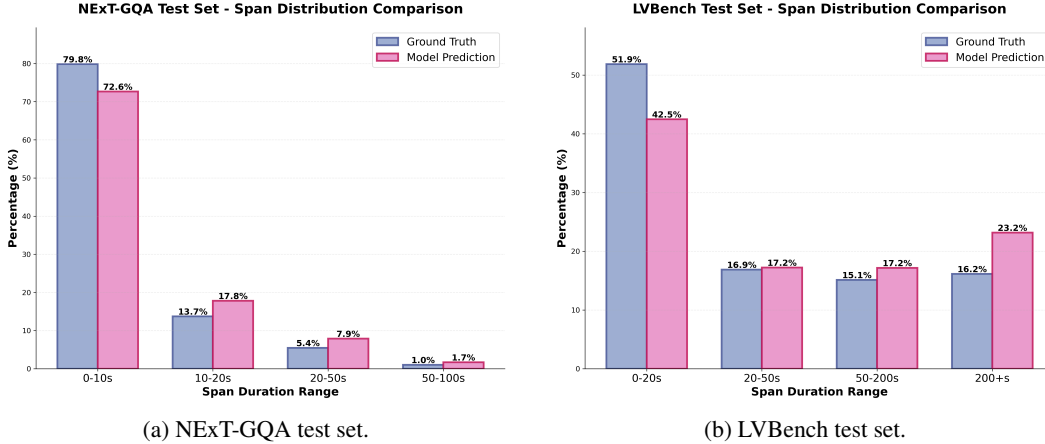


Figure B1: **Temporal span distribution comparison** between ground-truth annotations and model predictions. (a) NExT-GQA; (b) LVBench. Across both benchmarks, the model systematically shifts probability mass from shorter to longer spans, predicting broader temporal windows to capture sufficient contextual evidence for reasoning.

B Analysis of Temporal Span and FPS Prediction

We analyze the temporal span and FPS predictions of DynFrame to illustrate its learned retrieval behavior.

B.1 Temporal Span Prediction

Figure B1 compares the predicted and ground-truth span distributions on NExT-GQA (short-video) and LVBench (long-video). On NExT-GQA, ground-truth spans are heavily concentrated in the 0–10s range, and the model’s predictions closely follow this distribution while slightly redistributing mass toward longer spans, indicating accurate localization on short-form videos. On LVBench, where ground-truth spans are distributed more evenly across all duration ranges and are notably longer overall, the model consistently predicts correspondingly broader temporal windows for extended segments—mirroring the same adaptive behavior observed on shorter videos. This consistency across vastly different video lengths confirms that the model has learned a robust, duration-aware grounding strategy rather than a dataset-specific bias, with predictions shifting moderately toward wider windows to capture sufficient contextual evidence for downstream reasoning.

B.2 Dynamic FPS Prediction

Figure B2 shows the distribution of predicted retrieval FPS (f_2) of DynFrame. The majority of predictions fall within 1–4 fps. This concentration is well-aligned with the nature of most video understanding tasks, where moderate frame rates already provide sufficient visual information for accurate reasoning. Nevertheless, for highly dynamic scenes that demand dense temporal sampling to capture rapid changes within very short intervals, DynFrame also correctly predicts higher frame rates (5–6 fps), demonstrating its ability to adapt sampling density to content complexity.

To further investigate what drives different FPS predictions, we extract the most frequent content keywords within three FPS bands and visualize them as deduplicated word clouds (Figure B3). A clear semantic gradient emerges across the bands. **Low FPS (1–2 fps)** is dominated by static descriptors: *standing, wearing, background, shirt, wall, text*—scene descriptions and appearance attributes with minimal temporal variation. **Medium FPS (3–4 fps)** features sequential-activity terms: *around, begins, sequence, asks, observe*—multi-step procedures and conversational interactions that require tracking temporal progression but not rapid motion. **High FPS (5–6 fps)** is characterized by rapid-action keywords: *moving, throwing, jumping, collision, sphere, cube*—fast-paced physical interactions where dense sampling is essential to capture critical state transitions. This semantic stratification confirms that DynFrame learns a meaningful mapping from content dynamics to sampling frequency. Together with the span prediction strategy analyzed above, the two mechanisms work synergistically: broader spans increase temporal coverage, while adaptive FPS controls sampling density within the retrieved window.

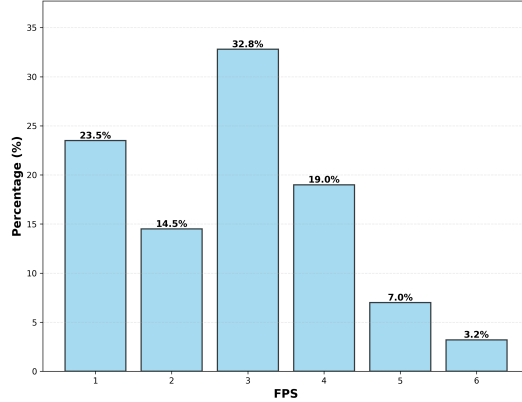


Figure B2: Predicted retrieval FPS distribution (f_2) of DynFrame.

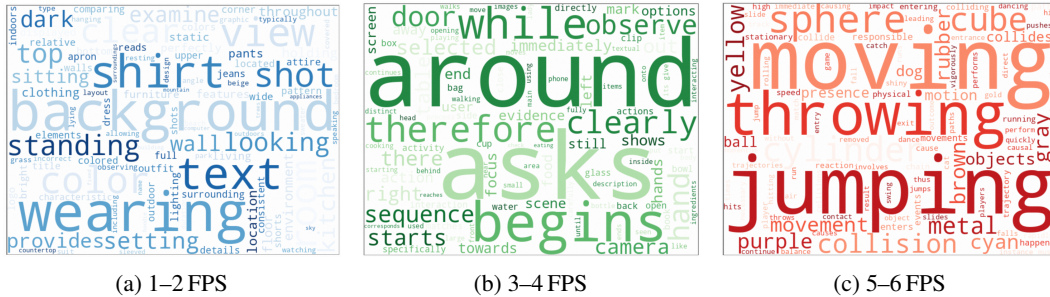


Figure B3: Word clouds of content keywords by retrieval FPS band. Low FPS captures static descriptors; medium FPS captures sequential activities; high FPS captures rapid actions.

C Frame-Budget and Context-Length Protocol

Table C1 reports the inference context protocol used by recent thinking-with-video methods and our **DynFrame**. We compare the average single-forward context length for each benchmark. Multi-round methods may additionally incur repeated forward calls and larger cumulative token costs.

Table C1: **Average single-forward context length across benchmarks.** Numbers are measured in tokens. “Max retrieval / injection” denotes the maximum number of visual revisiting operations used by each method: tool calls, zoom-in calls, iterative perception rounds, or visual-token injections. “0” indicates no visual retrieval after the initial input.

Model	Max retrieval / injection	Average single-forward context length					
		NExT-GQA	Charades	ActivityNet	Video-MME	MLVU	LVBench
Qwen2.5-VL-7B [2]	0	2910.9	1748.0	6282.4	2021.8	1991.5	2021.3
Video-R1-7B [6]	0	3893.2	3009.1	5482.5	4238.9	3968.4	4214.3
VideoZoomer [5]	4	12254.9	11195.1	11047.0	15745.0	17518.3	17896.7
Video-o3 [39]	8	55136.3	45716.0	44341.6	59134.0	61140.0	68478.1
VideoChat-R1.5-7B [35]	2	8897.5	5204.6	8213.9	38485.8	49872.9	46683.1
LongVT-RFT [36]	5	16389.0	10398.7	24113.6	33278.1	49606.9	55497.7
LOVE-R1-stage3 [8]	2	8480.5	4662.3	5757.5	10992.1	16919.5	18859.9
DynFrame-8B (ours)	1	6734.5	4936.7	5682.7	8253.7	7964.2	9749.6

Analysis. Table C1 shows that methods without visual retrieval have small and stable maximum contexts. Qwen2.5-VL-7B and Video-R1-7B require only one forward pass. For VideoZoomer and Video-o3, the official repositories enable multi-round visual revisiting: VideoZoomer uses up to four `<video_zoom>` calls, while Video-o3 uses up to eight `<grounding>` observations in its main multi-turn video-QA protocol. The corresponding rows are measured with these maximum retrieval trajectories rather than with single-turn Qwen-style context lengths.

In contrast, multi-round thinking-with-video systems substantially increase the average context length once retrieved visual evidence is inserted into the inference trajectory. VideoChat-R1.5, which uses iterative perception, reaches much larger contexts on long-form benchmarks such as Video-MME, MLVU, and LVBench. Tool-enabled LongVT-RFT further increases the maximum context length, especially on long-video tasks, because up to five retrieved clips can be appended across multiple

rounds. LOVE-R1 is lighter than LongVT-RFT-tool but still produces noticeably larger contexts than single-forward baselines due to its fast-view plus zoom-in reasoning design.

DynFrame follows a different design point. It uses only one model-predicted visual injection to jointly specify the temporal window and the sampling density. This makes each visual revisit more task-adaptive than fixed-policy retrieval calls. This design not only reduces the reliance on repeated retrieval rounds, but also improves accuracy over recent retrieval-based thinking-with-video methods on most evaluated benchmarks.

D Additional Qualitative Examples

We present additional qualitative examples to illustrate the behavior of DynFrame across diverse question types and video domains. Each example shows the model’s full reasoning trajectory, including the predicted temporal span, adaptive FPS selection, and the grounded answer derivation.

In the video, when the protagonist was grading the seventh test paper and calculating the scores, how many points did this test paper have? A. 58 points\nB. 48 points\nC. 52 points\nD. 60 points\nE. 50 points\nF. 54 points\nG. 56 points\n

Textual CoT

<think> I observe the protagonist grading papers with a red pen and moving through different test sheets. The relevant scoring action seems to **happen around 06:35-07:32**, where the hand is writing near the answer area. However, the page is partially occluded and the camera angle is unstable, so I assume this segment corresponds to the seventh test paper. In that moment, the red handwriting next to the multiple-choice section **looks like "83"** (the strokes appear like an "8" followed by a "3"), so I treat it as the recorded score/number for that question. **</think>**

<answer>Based on the visual progression .I conclude the protagonist wrote 83 for the seventh paper during 08:20-08:45, and the correct option should match that number. **</answer>**

✘

DynFrame

<think> The question asks for the score written on the seventh test paper. I need to locate the moment where they finish **scoring the seventh paper**. Starting around **08:20**, the person appears to have reached the seventh paper, moving the pen along marked sections and checking answers. **495.00-515.00 <fps>2</fps>**

In the selected segment, the person finishes marking the seventh test paper and writes a total score in red ink at the top right corner. The number written is **clearly '54'**, which is **then circled**, indicating the final score is 54 points. **\n</think> <answer>F</answer>**

✔

Figure D1: **Case study 1: long-video document counting.** DynFrame correctly identifies the 7th exam paper in the long video and accurately recognizes the scores in both grading rounds, whereas the textual CoT baseline fails.

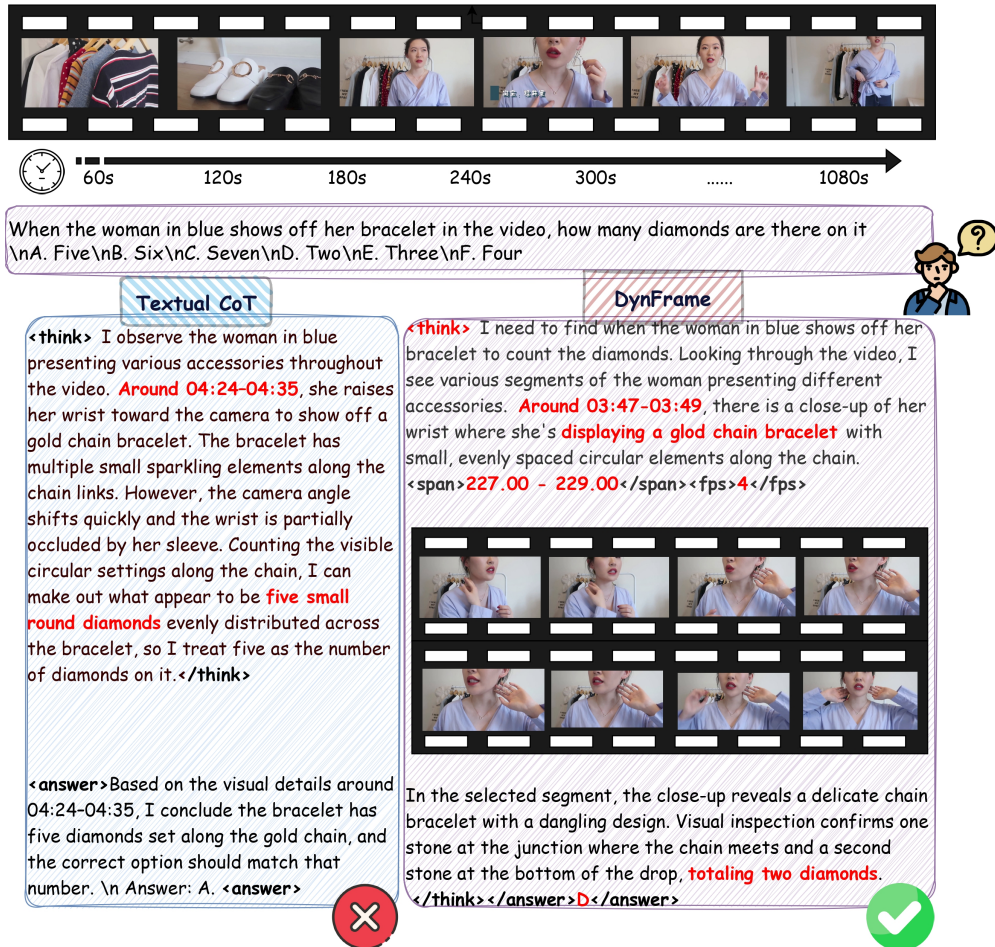


Figure D2: **Case study 2: fine-grained object counting.** DynFrame successfully locates the 2 s clip showcasing the bracelet in the long video and accurately counts the number of diamonds at 4 FPS, whereas the textual CoT baseline fails.